

# Flame Retardant Properties of a Guanidine Phosphate–Zinc Borate Composite Flame Retardant on Wood

Linyuan Wang,\* Yabing Yang, Hongbo Deng, Wenyi Duan, Jiajie Zhu, Yue Wei, and Wei Li



Cite This: *ACS Omega* 2021, 6, 11015–11024



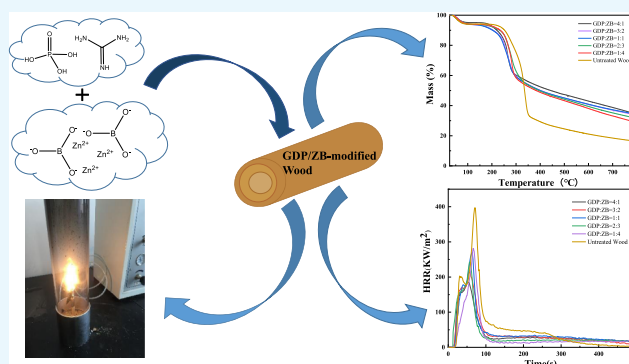
Read Online

ACCESS |

Metrics & More

Article Recommendations

**ABSTRACT:** This work combines guanidine dihydrogen phosphate (GDP) and zinc borate (ZB) to modify wood via microwave-ultrasonic impregnation for realizing favorable flame retardancy and thermal stability, which were investigated by the limiting oxygen index (LOI), thermogravimetric analysis (TGA), and cone calorimetry tests (CONE). The treated samples show better performance in fire retardancy with the LOI value increasing to 47.8%, and the results of TGA indicate the outstanding thermal stability of wood. In addition, the decline of heat release rate, total heat release, smoke production rate, and total smoke production examined by CONE further demonstrates the achievement of excellent flame retardancy and smoke suppression properties of the GDP/ZB-modified wood.



## 1. INTRODUCTION

As one of the four major raw materials, wood has been widely used in modern architecture and interior decoration due to its green environmental protection.<sup>1–3</sup> Wood is flammable and is mainly composed of three polymers, namely, cellulose, hemicellulose, and lignin. During combustion, wood releases considerable heat and produces a large amount of smoke, posing a threat to people's lives and properties.<sup>4–8</sup> Therefore, conducting flame retardant treatment on wood is urgent to reduce its flammability and protect people's lives. With the development of science and technology, research on flame retardants is focused on exploring a multieffect green flame retardant that is highly effective, nontoxic, harmless, safe, and environmentally friendly.<sup>9–12</sup>

The flame retardancy of wood can be traced back to the ancient Greeks, who impregnated wood with alum water to achieve the purpose of flame retardancy, which was also the first time in human history that a wood flame retardant was applied in the military field.<sup>13</sup> Subsequently, the exploration of wood flame retardants has become increasingly systematic. In accordance with the type of compound, flame retardants can be divided into organic and inorganic flame retardants. At present, the commonly used organic flame retardants are mainly organic compounds of elements, such as nitrogen, phosphorus, and bromine.<sup>14–16</sup> However, out of consideration for the environment in recent years, halogen flame retardants have been abandoned due to a large amount of smoke and harmful gases released during combustion.<sup>17–20</sup> Nitrogen and phosphorus flame retardants have been gradually and widely used due to their good flame retardant effect and minimal

smoke.<sup>21–23</sup> Alumina hydroxide, magnesium hydroxide, and zinc borate (ZB) are the typical representatives of inorganic flame retardants, which are frequently used due to their smokeless, nontoxic, high safety, and low price characteristics.<sup>24,25</sup> Guanidine phosphate (GP) was first synthesized by a Japanese scholar Kiichiro Sugino in 1938. It has been widely used in flame retardant products, such as wood and paper, due to its economical applicability and good flame retardant effect.<sup>26–30</sup> Goldstein<sup>31</sup> reacted dicyandiamide aqueous solution with equal molar phosphoric acid to generate transparent amidinourea phosphate. This solution was used to impregnate wood for improving flame retardancy and moisture absorption. Zhou synthesized GP by referring to the method of Cummins.<sup>32</sup> This synthesized solution was used as the flame retardant of paper and fiber materials. ZB is a widely used inorganic flame retardant additive with nontoxic, nonpolluting, smoke-suppressing features.<sup>33</sup> B. Garba<sup>34</sup> used a diluted hydrochloric acid solution of ZB as a wood impregnation solution. The flame retardant characterization test showed that ZB can effectively reduce flame propagation speed and ignition time, thereby improving the limiting oxygen index (LOI) value and carbon formation rate. Hu<sup>35</sup> synthesized ZB through solid-

Received: February 18, 2021

Accepted: April 6, 2021

Published: April 17, 2021



phase synthesis and explored the effect of its combination with ammonium polyphosphate on the thermal stability of wood flour. The results showed that the combination of the two compounds increased the char formation rate of wood flour, showing a good flame retardancy. However, adding a large proportion of compounds is usually necessary to achieve the corresponding flame retardant effect.<sup>36</sup> This condition is due to the chemical structure of inorganic flame retardants. Achieving the expected effect with a single flame retardant is difficult. Therefore, a mixed flame retardant is selected to prevent wood burning and smoke generation by using the synergistic effect between flame retardants.

In the present work, we dissolve guanidine dihydrogen phosphate (GDP) and ZB using a diluted phosphoric acid. The solution is prepared into different proportions of composite mixed impregnation solution to treat wood through microwave-ultrasonic impregnation. This process is performed to improve the flame retardant performance of wood, protect the environment, and reduce the generation of toxic and harmful gases. The performance indicators of untreated wood and GDP/ZB flame retardant wood are investigated through the muffle furnace test, limiting oxygen index (LOI), thermogravimetric analysis (TGA), cone calorimetry burning test (CONE), and scanning electron microscopy (SEM).

This work aims to explore the compound synergistic effect of GDP and ZB. The synergistic flame retardant mechanism is discussed to improve the flame retardant performance of wood while reducing the amount of smoke.

## 2. RESULTS AND DISCUSSION

**2.1. Effect of Reaction Temperature and Time on the Yield of GP.** When dicyandiamide and ammonium chloride are used to synthesize guanidine phosphate (GP) with a molar ratio of 1:2, the final yield of GP will be affected by the temperature and time in the reaction process. GDP and diguanidine hydrogen phosphate (DHP) were synthesized at certain temperatures (170 °C, 190 °C, 210 °C, and 230 °C) for different hours (2 h, 2.5 h, and 3 h). The yields of the synthesized products are shown in Table 1.

It can be seen from Table 1 that the yields of GDP and DHP at different temperatures and different times are not the same, with some differences. The yields of synthetic products generally show an increasing trend with the increase of time and temperature. Compared with time, the temperature has a

greater impact on the synthesis yield of guanidine phosphate. Under the same reaction conditions, the yield of GDP is slightly higher than that of DHP. When the reaction temperature is 230 °C and the reaction time is 2.5 h, the yields of GDP and DHP are both the highest, reaching 83.49% (GDP) and 82.77% (DHP), respectively.

When dicyandiamide and ammonium chloride are used to synthesize GDP and DHP at a ratio of 1:2, the synthesis yields are the highest under the reaction conditions of 230 °C for 2.5 h, which is the optimal synthesis reaction condition.

**2.2. Fourier Transform Infrared Spectra Analysis.** As observed in Figure 1a,b, the N–H association bond in guanidine  $\text{H}_2\text{NC}(=\text{NH})\text{NH}_2$  has a wide and strong absorption peak in the range of 3500–3100  $\text{cm}^{-1}$  due to stretching vibration. Another weak absorption peak caused by the absorption of the P–OH bond in GP appears at approximately 2402  $\text{cm}^{-1}$ . A strong absorption peak caused by the stretching vibration of the C=N double bond in the guanidine group occurs at approximately 1664.2  $\text{cm}^{-1}$ . The flexural vibration peak caused by the N–H bond of the primary amine in guanidine appears at approximately 1585.1  $\text{cm}^{-1}$ .<sup>26</sup> Comparing Figure 1a,b with the infrared spectra of standard GP, the absorption peaks and absorption intensities in the range of 1300–800  $\text{cm}^{-1}$  are the same. These peaks and intensities are caused by the stretching vibration of the P–O bond in  $\text{H}_2\text{PO}_4^-$ .<sup>28</sup>

**2.3. Muffle Furnace Burning Analysis.** The carbon residue rate of GP is shown in Table 2 and Figure 2. The results show that the carbon residue rate of untreated wood flour is 26.76%, and the weight loss rate is 73.24%. The carbon residue rate of GDP is 47.64%, and the weight loss rate is 52.36%. The carbon residue rate of DHP is 45.89%, and the weight loss rate is 54.11%. GDP and DHP have a certain flame retardant effect. The carbon residual rate of GDP increases by 20.88% and 19.13% compared with the control group. The carbon residual rate of GDP is 1.75% higher than that of DHP, indicating that the flame retardant effect of GDP is better than that of DHP. Thus, choosing GDP as the main agent of the composite flame retardant system is appropriate.

The composition of ultrafine ZB has a certain effect on the flame retardancy of wood.<sup>35</sup> Accurately weighed 0.100 g of ZB was mixed in accordance with the molar ratio of zinc oxide to boric acid as 1:1, 1:2, 1:3, 2:1, and 3:1. The five mixtures were placed in the crucibles containing 0.900 g of wood flour. The five crucibles were placed into the muffle furnace and marked as A1–A5. The five crucibles were cooled to room temperature and weighed after 40 min burning at a constant temperature of 400 °C. Their residual weights were recorded to calculate the carbon residual rate. The results are reported in Table 3.

From Figure 3, the higher the carbon residue rate of wood flour, the more effective the flame retardant effect. When the molar ratio of zinc oxide and boric acid was 1:1 for solid-phase synthesis of ZB, the wood powder was burned in the muffle furnace with the maximum residual weight. The residual carbon rate reaches 42.46%, and the flame retardant effect is the best. Therefore, ZB has high flame retardant performance when it is synthesized by the solid phase of zinc oxide and boric acid with a molar ratio of 1:1.

**2.4. SEM–EDS Analysis.** Scanning electron microscopy coupled with energy-dispersive spectroscopy (SEM–EDS) is used to confirm the dispersion of GDP/ZB in the wood substrate.

**Table 1. Yields of GP at Different Temperatures and Different Times**

sample	reaction temperature (°C)	reaction time (h)	GDP yield/%	DHP yield/%
1	170	2	73.06	73.00
2		2.5	74.65	73.97
3		3	75.78	74.78
4	190	2	73.11	73.09
5		2.5	76.20	75.12
6		3	77.93	77.52
7	210	2	80.13	79.97
8		2.5	81.67	81.03
9		3	82.38	82.17
10	230	2	82.33	81.73
11		2.5	83.49	82.77
12		3	83.46	82.38

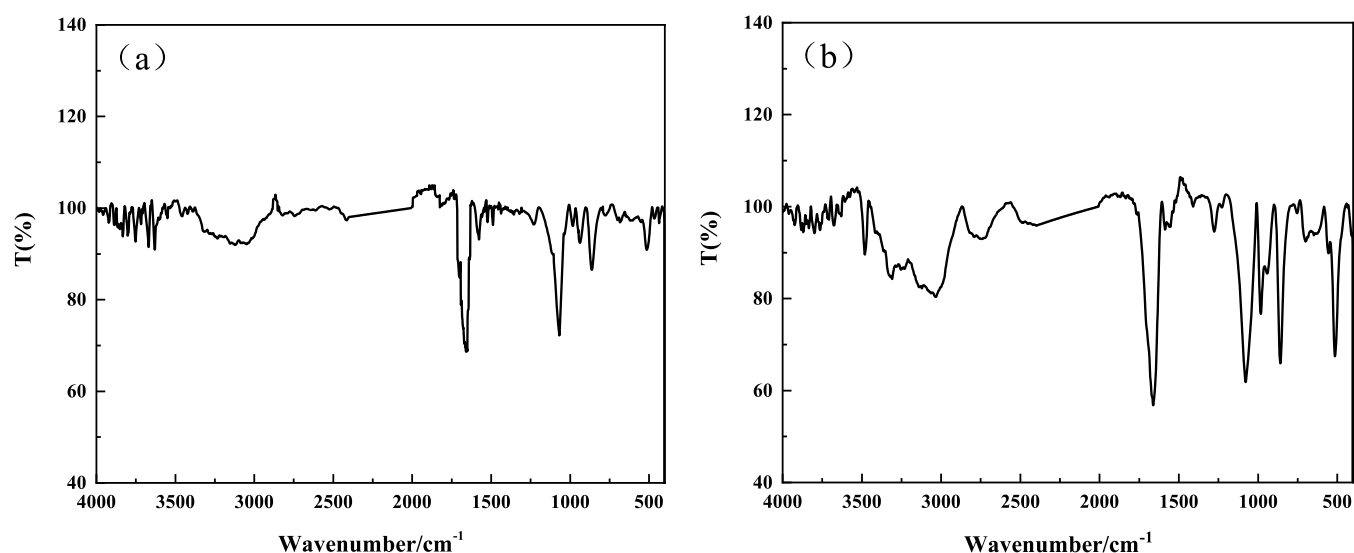


Figure 1. (a) Infrared spectra of GDP and (b) infrared spectra of DHP.

Table 2. Results of the Carbon Residue Rate of Wood Flour

sample	wood (g)	GP (g)	carbon residue rate/%	weight loss rate/%
GDP	0.900	0.100	47.64	52.36
DHP	0.900	0.100	45.89	54.11
UW	1.000	0.000	26.76	73.24

The corresponding main elemental composition and distribution of the GDP/ZB flame retardant located on the cell structure of the wood are shown in Figure 4. From the elemental mapping images, the P, Zn, B, and N elements are the four main elements of the GDP/ZB composite flame retardant and distributed homogeneously inside the GDP/ZB-modified wood via impregnation. The uniform distribution of the four main elements proves that GDP/ZB has entered the wood.

**2.5. Limiting Oxygen Index Analysis.** From Table 4, it can be seen that untreated wood is an extremely flammable substance with an LOI value of only 22.4%. The LOI value of flame retardant wood treated with GDP significantly increases, and the LOI value increases with the increase in the mass

Table 3. Carbon Residue Rates of ZB with Different Compositions

sample	wood (g)	ZB (g)	ZnO: H <sub>3</sub> BO <sub>3</sub>	carbon residue rate/%
A1	0.900	0.100	1:3	37.94
A2	0.900	0.100	1:2	39.91
A3	0.900	0.100	1:1	42.46
A4	0.900	0.100	2:1	41.24
A5	0.900	0.100	3:1	39.77

fraction of the GDP flame retardant. When the mass fraction of flame retardant is 10%, the LOI value is 43.4%, which is 93.75% higher than that of untreated wood. Therefore, the GDP flame retardant has a good flame retardant effect in the wood application.

Table 5 shows the LOI values of flame retardant wood with different formulas when the mass fraction of the GDP/ZB composite flame retardant is 10%. From the data in Table 5, the LOI values of wood after flame retardant treatment are significantly increased. The LOI values of wood after composite treatment of GDP and ZB are higher than that

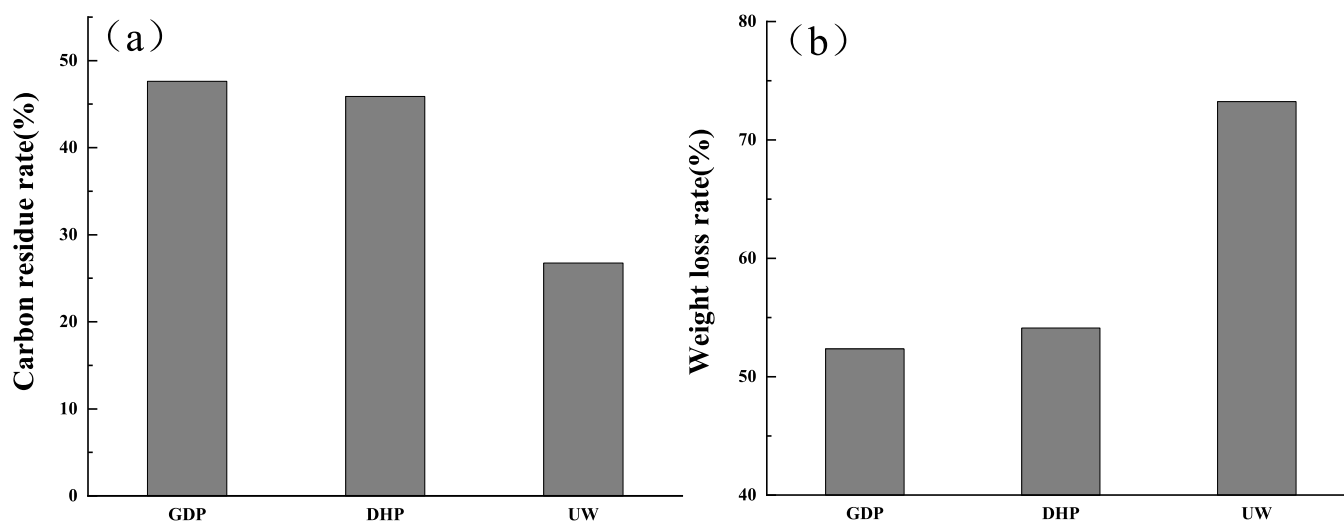


Figure 2. (a) Carbon Residual Rate of Wood Flour. (b) Weight Loss Rate of Wood Flour.

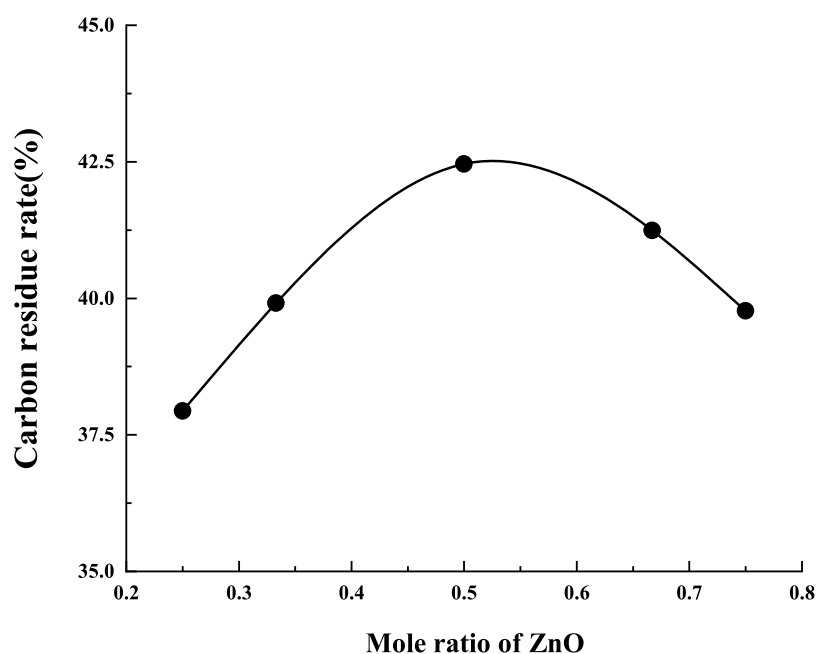


Figure 3. Carbon Residue Rates of ZB with Different Compositions.

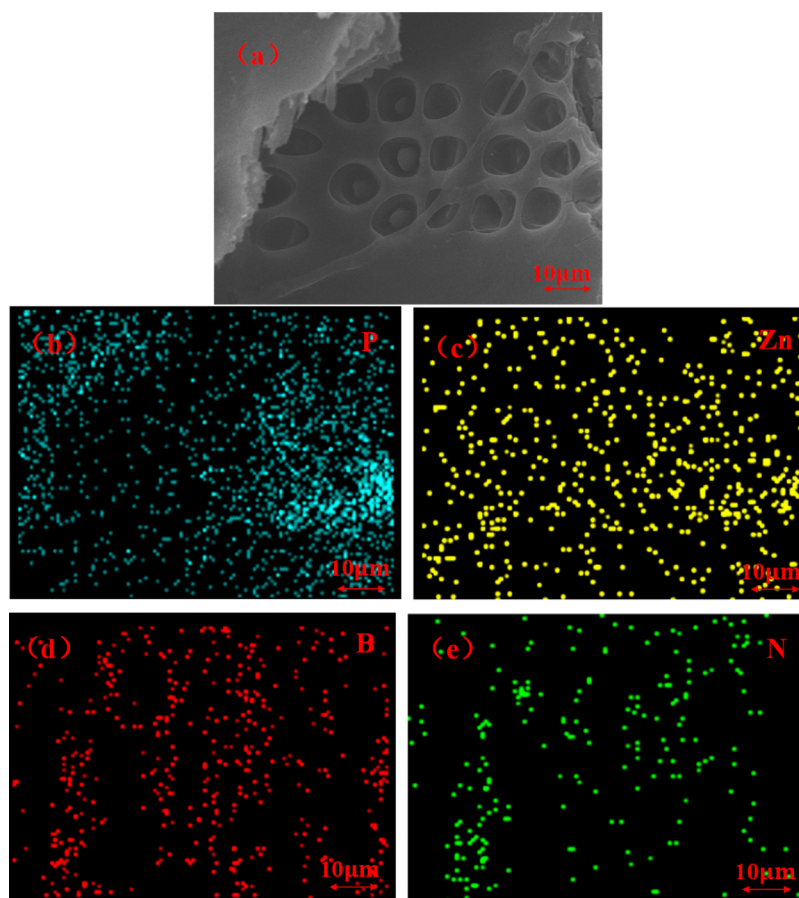


Figure 4. (a) Cross-sectional SEM images of GDP/ZB-modified wood and (b–e) corresponding elemental mapping images of P, Zn, B, and N elements.

with a single flame retardant treatment. The LOI values of composite flame retardant wood increase with the increase in GDP content. When GDP: ZB = 4:1, the LOI value of GDP/ZB flame retardant wood is the highest, reaching 47.8%, which

is 113.39% higher than that of untreated wood. Compared with GDP and ZB flame retardants, the LOI value of GDP/ZB flame retardant wood is greatly improved, increasing by 10.14% and 66.55%. Thus, GDP and ZB have good synergistic

Table 4. LOI Values of GDP Flame Retardant Wood

sample	GDP (wt %)	LOI (%)
B0	UW	22.4
B1	2.00	28.2
B2	4.00	31.8
B3	6.00	35.7
B4	8.00	39.6
B5	10.00	43.4

Table 5. LOI Value of GDP/ZB Composite Flame Retardant Wood

formulation	GDP (wt %)	LOI (%)
untreated wood	UW	22.4
GDP/ZB = 1:0	10.00	43.4
GDP/ZB = 4:1	10.00	47.8
GDP/ZB = 3:2	10.00	47.3
GDP/ZB = 1:1	10.00	46.6
GDP/ZB = 2:3	10.00	46.4
GDP/ZB = 1:4	10.00	46.0
GDP/ZB = 0:1	10.00	28.7

effects, and their combination can provide a better flame retardant effect.

**2.6. Thermogravimetric Analysis.** The TGA results of the GDP/ZB composite flame retardant wood and untreated wood in a nitrogen protected atmosphere are shown in Figure 5. From TGA and DTG curves shown in Figure 5a,b, respectively, it can be seen that the thermal weight loss trends of untreated wood and GDP/ZB composite flame retardant wood are the same.

The pyrolysis of untreated wood is mainly divided into the following three stages. The first stage occurs between 100 and 120 °C due to the evaporation of moisture from the wood, causing 6.37 wt % mass loss. The second stage occurs within the temperature range from 200 to 360 °C, which is also the main pyrolysis stage of the wood. The decomposition of the wood constituents (lignin, cellulose, and hemicelluloses) can release considerable heat and produce CO, CO<sub>2</sub>, CH<sub>4</sub>, and other pyrolysis gases,<sup>37</sup> causing 68.14 wt % mass loss. The third

stage occurs after 360 °C with the carbonization of lignin, which can form char layers, causing 9.62 wt % mass loss.

From the TGA curves in Figure 5a, the initial decomposition temperature of the wood treated by the GDP/ZB composite flame retardant is lower than that of the untreated wood. When GDP: ZB = 4:1, the initial decomposition temperature decreases from 213.83 to 162.33 °C, which is probably due to the catalytic degradation of cellulose caused by GDP/ZB.<sup>38</sup> For GDP: ZB = 4:1, the char residuals increase to 37.83%, which is much higher than that of an untreated wood (16.27%), exhibiting the highest residual weight among the samples. Lower initial decomposition temperature and the increase of char residuals indicate that the addition of GDP/ZB can promote the formation of the charring layer at lower temperatures,<sup>39</sup> preventing further decomposition.

From the DTG curves in Figure 5b, the maximum decomposition rate and the temperature of maximum weight loss rate of GDP/ZB-modified wood both show downward trends. When GDP: ZB = 4:1, the prominent peak shifted to the lowest temperature at 264.17 °C, which is 70.50 °C lower than that of the untreated wood. The addition of the GDP/ZB can change the thermal degradation behavior of wood and reduce the temperature of maximum weight loss rate, leading to formation of more char residuals.<sup>40</sup>

Comparing the GDP/ZB composite flame retardant wood and untreated wood in TGA and DTG curves, the initial decomposition temperature and the temperature of maximum weight loss rate of untreated wood are higher than those of the GDP/ZB-modified wood, which indicates that the combination of GDP and ZB can slow down the thermal degradation of wood and promote the char formation, which can prevent thermal conduction and further protect the wood from decomposition.

**2.7. Cone Calorimetric Analysis.** The cone calorimetry test can objectively evaluate the flame performance of wood when an actual fire occurs. The flame retardancy of wood is evaluated by measuring the heat release rate (HRR), peak heat release rate (PHRR), and total heat release (THR). The smoke emission capacity of wood combustion is evaluated by measuring the smoke production rate (SPR) and total smoke production (TSP).<sup>41</sup>

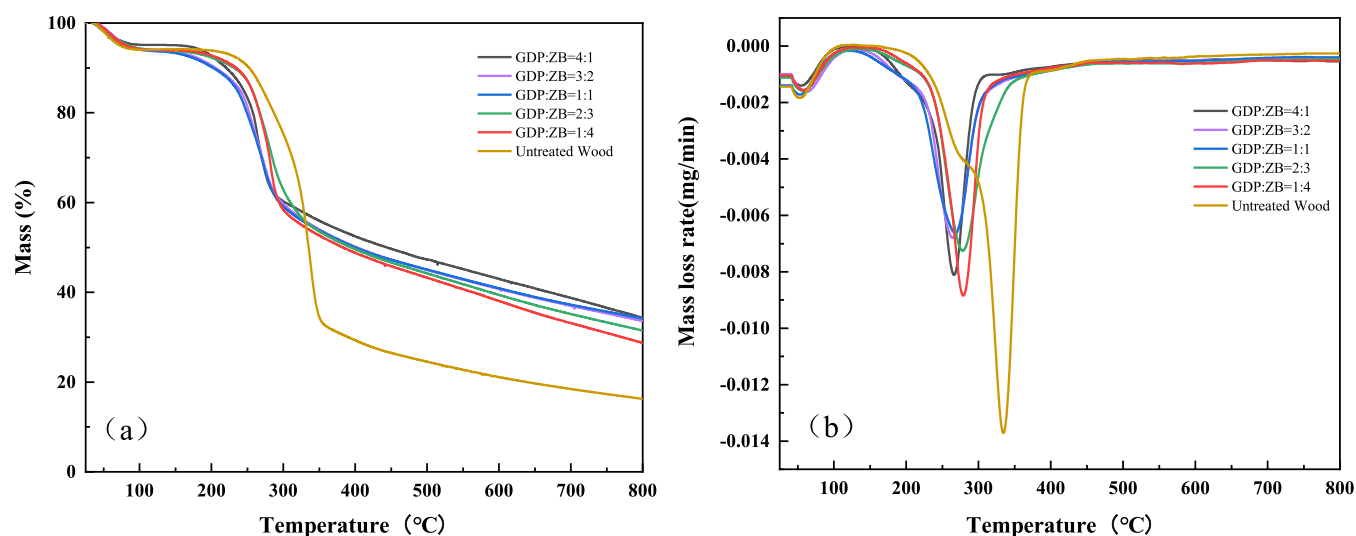


Figure 5. (a) TGA curves of untreated wood and composite wood and (b) DTG curves of untreated wood and composite wood.

Figure 6 shows the HRR of GDP/ZB composite flame retardant wood and untreated wood. As shown in Figure 6, the

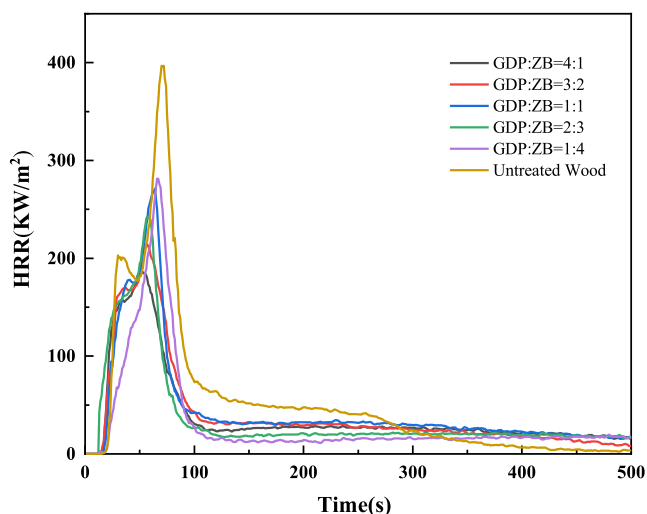


Figure 6. HRR as a function of time.

HRR curves of wood are bimodal, and the second exothermic peak is sharper, which is the main decomposition stage of wood. The shape of the HRR curves of GDP/ZB composite flame retardant wood shows a tendency similar to that of untreated wood. The positions of the first and second exothermic peaks of modified wood are slightly advanced, and the peak values are obviously reduced. The PHRR of untreated wood is 396.28 kW/m<sup>2</sup>. With the increase in GDP content, the PHRR decreases. When GDP: ZB = 4:1, the PHRR drops to the lowest level, with only 186.19 kW/m<sup>2</sup>, a decrease of 210.09 kW/m<sup>2</sup>, which is only 46.98% of untreated wood.

Figure 7 shows the THR of GDP/ZB composite flame retardant wood and untreated wood. As shown in Figure 7, the THR values of the GDP/ZB-modified wood are significantly lowered compared with that of untreated wood (27.24 MJ/m<sup>2</sup>). With the increase in GDP, the THR decreased continuously. When GDP: ZB = 4:1, the minimum value of

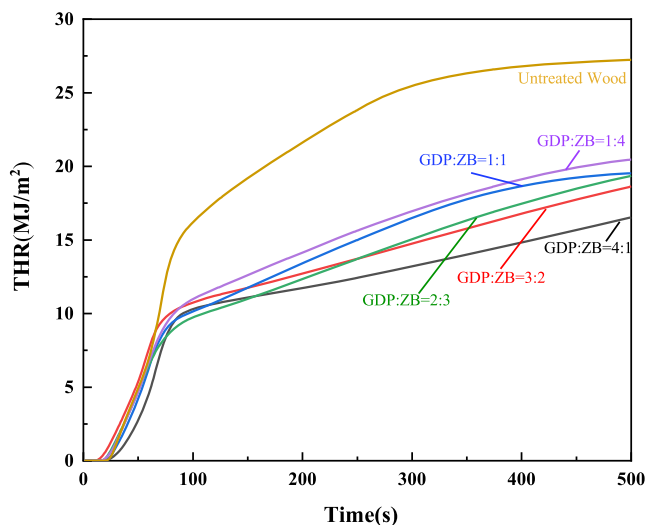


Figure 7. THR as a function of time.

THR is 16.54 MJ/m<sup>2</sup>, which is only 60.72% of that of untreated wood.

As shown in the HRR and THR curves, GDP and ZB have certain flame retardant effects on wood. Compared with untreated wood, the composite flame retardant wood has a lower value of PHRR and THR. These findings indicate that the composite flame retardant can provide a better synergistic flame retardant effect. The increase content of flame retardant GDP can significantly reduce the PHRR and THR of wood, thereby showing better flame retardant performance.

Figure 8 shows the SPR of GDP/ZB composite flame retardant wood and untreated wood. As shown in Figure 8, the

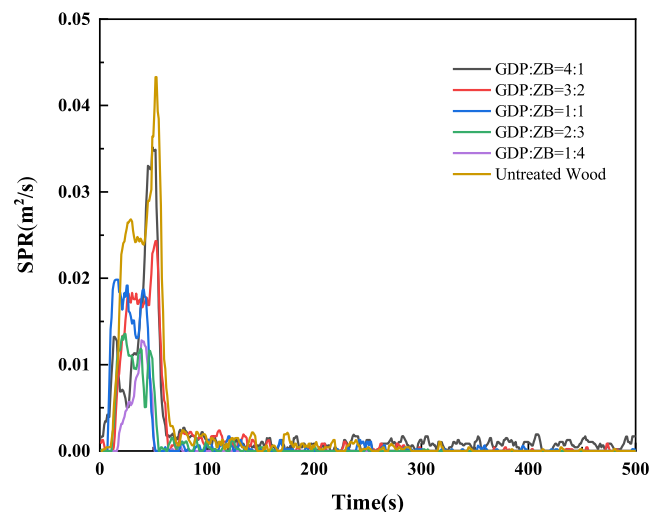


Figure 8. Smoke produce rate (SPR) as a function of time.

SPR curves of wood have two obvious peaks, and the second SPR peak is sharper. The SPR peak of untreated wood is 0.043 m<sup>2</sup>/s, which is much higher than that of composite flame retardant wood. With the increase in ZB content, the SRR peak decreases. When GDP:ZB = 1:4, the minimum value of the SRR peak is 0.013 m<sup>2</sup>/s, which is 0.03 m<sup>2</sup>/s lower than that of untreated wood.

Figure 9 shows the TSP of GDP/ZB composite flame retardant wood and untreated wood. As shown in Figure 9, the

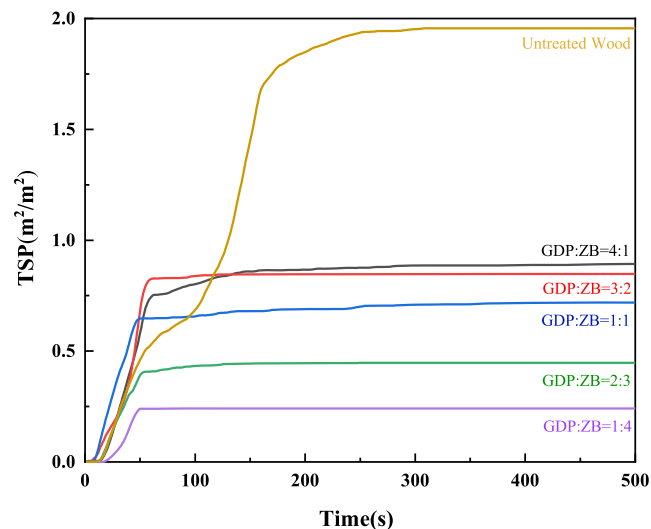


Figure 9. TSP as a function of time.

TSP of wood treated with GDP/ZB composite flame retardant reduces to a different extent. Untreated wood can emit smoke continuously and rapidly for a long period of time, and the TSP can reach 1.96 m<sup>2</sup>/m<sup>2</sup>. The TSP of the GDP/ZB composite flame retardant decreases with the increase in ZB content, and the time for producing smoke is shortened. After 250 s, the smoke production gradually becomes flat. When GDP: ZB = 1:4, the TSP is at least 0.24 m<sup>2</sup>/m<sup>2</sup>, which is 1.72 m<sup>2</sup>/m<sup>2</sup> lower than that of untreated wood and is 12.24% of that of untreated wood.

As shown in the SPR and TSP curves, ZB has a better smoke suppression performance than GDP when the combination of GDP and ZB played a synergistic flame retardant role. The increase in the content of ZB can shorten the smoke generation time and reduce the total smoke generation. In the initial stage of wood ignition, the ZB flame retardant can promote dehydration into charcoal and release crystal water to dilute combustible components. After melting at high temperature, it covers the wood surface to form a protective film, thereby inhibiting the generation of harmful gases and exerting a significant smoke-suppressing effect.<sup>42</sup>

The toxic and harmful gases released in the process of wood combustion can cause deaths. Therefore, the yield of toxic and harmful gases is also an important indicator for evaluating the burning behavior of wood.<sup>43</sup> Carbon monoxide is the main toxic and harmful gas released during the burning process. People are prone to be poisoned with the increase of the carbon monoxide yield (defined as the mass of CO formed from the unit mass of burned material).<sup>44</sup> Table 6 shows the results of mean-CO yield (kg/kg) and the peak-CO yield of GDP/ZB-modified wood and untreated wood.

**Table 6. Results of CO Yield**

formulation	mean-CO yield (kg/kg)	peak-CO yield (kg/kg)
untreated wood	0.0216	0.0831
GDP/ZB = 4:1	0.0103	0.0625
GDP/ZB = 3:2	0.0068	0.0400
GDP/ZB = 1:1	0.0045	0.0222
GDP/ZB = 2:3	0.0024	0.0189
GDP/ZB = 1:4	0.0020	0.0179

It can be seen from Table 6 that the mean-CO yield and peak-CO yield of GDP/ZB-modified wood both decrease compared with untreated wood. When GDP/ZB = 1:4, the minimum value of the mean-CO yield (kg/kg) is 0.0020 (kg/kg), which is 90.74% lower than untreated wood, while the peak-CO also drops from 0.0831 (kg/kg) to 0.0179 (kg/kg). The decline of the mean-CO yield and peak-CO yield represent the reduction in the amount of toxic and harmful gases during the burning process of the material, indicating that the introduction of GDP/ZB plays a role in smoke suppression on the wood.

**2.8. Scanning Electron Microscopy.** The wood burned by CONE is observed through SEM to better observe the morphology of carbon residues in the combustion of untreated wood and GDP/ZB composite wood. As shown in Figure 10, untreated wood becomes wood ash after burning, and its internal structure is incomplete, presenting a soft and expanding flocculent structure. The GDP/ZB composite wood is burned to form charcoal. The relatively complete dense carbon layer structure is still intact, and the fiber skeleton structure of the wood can also be seen.<sup>45</sup> In the

combustion of the flame retardant wood, GDP and ZB had a synergistic flame retardant effect, forming a covering layer on the wood surface. This effect effectively prevented the burning of the wood and achieved the purpose of flame retardancy.

### 3. CONCLUSIONS

In this work, we prepared an impregnating solution combining GDP and ZB to modify wood by microwave-ultrasonic treatment. The effect of the GDP/ZB composite flame retardant on flame retardant properties of wood was evaluated. In detail, the LOI value of the wood increased from 22.4% to 47.8%, indicating the enhancement of the fire performance of the GDP/ZB-modified wood. From the TGA test, it can be seen that the initial decomposition temperature and the temperature of maximum weight loss rate decreased to 162.33 °C and 264.17 °C, respectively, with the increase of the char residual. Moreover, cone calorimetry tests show that the increase in GDP concentration can significantly reduce HRR and THR. In contrast, the increase in the content of ZB can effectively suppress the generation of smoke. The above results proved that the GDP/ZB composite flame retardant not only improves the flame retardancy and thermal stability of the wood but also inhibits the generation of toxic and harmful smoke.

### 4. EXPERIMENTAL SECTION

**4.1. Materials.** Dicyandiamide, ammonium chloride, sodium hydroxide, methanol, and phosphoric acid (≥85%) were purchased from Kelong Chemical Reagent Co. (Chengdu, China). Zinc oxide and boric acid were provided by Zhiyuan Chemical Reagent Co., Ltd. (Tianjin, China). Wood was supplied by Southwest Building Materials (Chengdu, China).

**4.2. Guanidine Phosphate Synthesis.** At atmospheric pressure, dicyandiamide and ammonium chloride were melted at 170–230 °C with a mole ratio of 1:2 for 2–3 h. Methanol and flaky solid sodium hydroxide were sequentially added after cooling to room temperature. The reacted solution was then filtered after stirring and refluxing for 2 h. The filtrate was neutralized with 85% phosphoric acid.<sup>29</sup> When the pH value was 8, the white precipitate of DHP was obtained. When the pH value was 4, the white precipitate of GDP was obtained. The white powder of GDP or DHP was obtained after precipitation aging, suction filtration, and drying.

**4.3. Preparation of ZB.** On the basis of solid-phase synthesis, boric acid and zinc oxide with a certain weight are weighed in accordance with the formula in Table 3. Zinc oxide and boric acid were triturated in an agate mortar for 40 min. They were then evenly mixed and ground in the mortar for at least 40 min until uniform to prepare ultrafine ZB with different compositions.<sup>35</sup>

**4.4. Preparation of the GDP–ZB Complex System.** The total mass fraction of the compound flame retardant was controlled to 10%. The mixture ratio of GDP and ZB was changed in accordance with the formula in Table 5 to prepare an impregnation solution with diluted phosphoric acid for reserve.

**4.5. Wood Sample Preparation.** Naturally grown poplar wood was cut into the required size and dried at 105 °C for 8 h to reach a moisture content less than 2%. In accordance with the formula in Tables 4 and 5, the samples were treated at 850 W microwave power for 1.5 min and then immediately put into

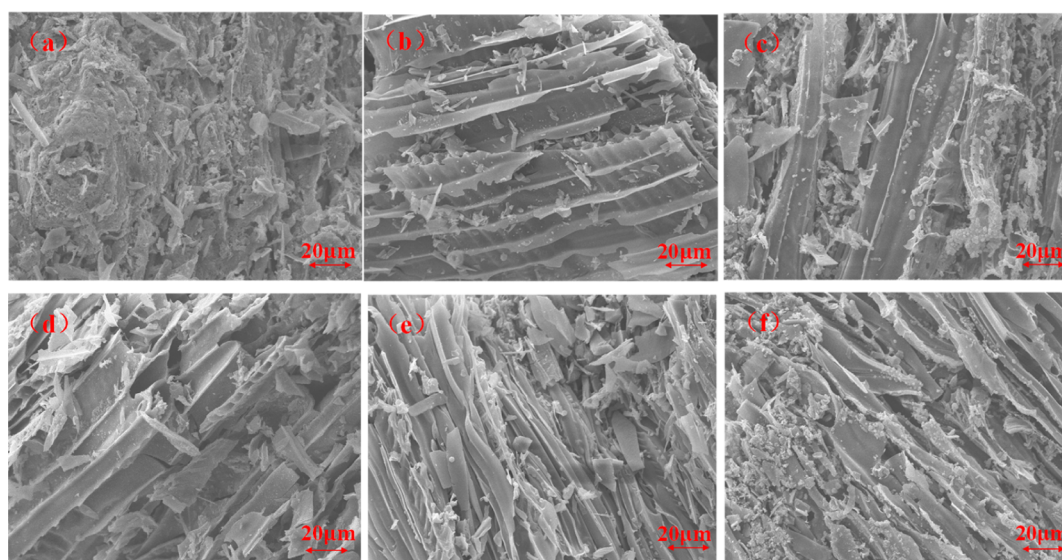


**Figure 10.** SEM of the carbon residue of untreated wood and composite wood, (a) untreated wood, (b) GDP/ZB = 4:1, (c) GDP/ZB = 3:2, (d) GDP/ZB = 1:1, (e) GDP/ZB = 2:3, and (f) GDP/ZB = 1:4.

an ultrasonic instrument filled with flame retardant solution under 500 W ultrasonic power and 60 °C for 40 min with microwave treatment.

**4.6. Measurements.** **4.6.1. Fourier Transform Infrared Spectra.** A WQF-520 Fourier infrared spectrometer (Beijing Ruili Analytical Instrument Co., Ltd, China) was used to test the sample functional groups by using the KBr tableting method. The scanning range was 4000–400  $\text{cm}^{-1}$  in the midinfrared region, and the resolution was 4  $\text{cm}^{-1}$  with 16 scanning times.

**4.6.2. Muffle Furnace Burning.** An FP-40 ceramic fiber muffle furnace (Shanghai Chemical Branch, China) was used to conduct the charcoal burning experiment. In accordance with the formula in Tables 2 and 3, GP and ZB were mixed evenly with wood powder in porcelain crucibles and were then placed into a muffle furnace burning at a constant temperature of 400 °C for 40 min.

**4.6.3. Limiting Oxygen Index.** In accordance with the ASTM D2863-97 standard, a DRK304B oxygen index tester (Shandong Drake Instrument Co., Ltd, China) was used to test the LOI values and measure the combustion behavior of the samples. The sample size was 120 mm  $\times$  10 mm  $\times$  4 mm.

**4.6.4. Thermogravimetry.** A STA449F3 thermogravimetric analyzer (Netzsch, Germany) was used to test the thermal stability properties of the samples. The weights of all samples were kept within 5–8 mg in alumina crucibles with lids. The test temperature ranged from 25 to 800 °C with a heating rate of 10 °C/min under the  $\text{N}_2$  atmosphere.

**4.6.5. Cone Calorimetry.** In accordance with ISO 5660-1:2002, a CCT cone calorimeter (Kunshan Modisco Combustion Technology Instrument Co., Ltd., China) was used to measure the combustion performance of the samples. The thermal radiation power was 50  $\text{kW/m}^2$ . The sample sizes were 100 mm  $\times$  100 mm  $\times$  10 mm.

**4.6.6. Scanning Electron Microscopy.** A ZEISS EV0 MA15 scanning electron microscope (Carl Zeiss, Germany) was used to observe the surface morphology of the samples. The residual carbon surface of the samples after the cone calorimeter burning test was sprayed with gold.

## AUTHOR INFORMATION

### Corresponding Author

Linyuan Wang – School of Chemistry and Chemical Engineering, Southwest Petroleum University, Chengdu 610500, China; [orcid.org/0000-0003-3955-453X](https://orcid.org/0000-0003-3955-453X); Email: 13981884015@163.com

### Authors

Yabing Yang – School of Chemistry and Chemical Engineering, Southwest Petroleum University, Chengdu 610500, China

Hongbo Deng – School of Chemistry and Chemical Engineering, Southwest Petroleum University, Chengdu 610500, China

Wenyi Duan – School of Chemistry and Chemical Engineering, Southwest Petroleum University, Chengdu 610500, China

Jiajie Zhu – School of Chemistry and Chemical Engineering, Southwest Petroleum University, Chengdu 610500, China

Yue Wei – School of Chemistry and Chemical Engineering, Southwest Petroleum University, Chengdu 610500, China

Wei Li – Fourth Oil Production Plant of Qinghai Oilfield, China National Petroleum Corporation, Jiuquan 736202, China

Complete contact information is available at:  
<https://pubs.acs.org/10.1021/acsomega.1c00882>

### Notes

The authors declare no competing financial interest.

## ACKNOWLEDGMENTS

This work was financially supported by National Natural Science Foundation of China (Grant no. 51704248).

## REFERENCES

- Wimmers, G. Wood: a construction material for tall buildings. *Nat. Rev. Mater.* **2017**, *2*, 51.
- Zhu, H.; Luo, W.; Ciesielski, P. N.; Fang, Z.; Zhu, J. Y.; Henriksson, G.; Himmel, M. E.; Hu, L. Wood-Derived Materials for

Green Electronics, Biological Devices, and Energy Applications. *Chem. Rev.* **2016**, *116*, 9305–9374.

(3) Guo, H.; Özparpucu, M.; Windeisen-Holzhauser, E.; Schlepütz, C. M.; Quadranti, E.; Gaan, S.; Dreimol, C.; Burgert, I. Struvite Mineralized Wood as Sustainable Building Material: Mechanical and Combustion Behavior. *ACS Sustainable Chem. Eng.* **2020**, *8*, 10402–10412.

(4) Kandola, B. K.; Horrocks, A. R.; Price, D.; Coleman, G. V. Flame-Retardant Treatments of Cellulose and Their Influence on the Mechanism of Cellulose Pyrolysis. *J. Macromol. Sci., Polym. Rev.* **1996**, *36*, 721–794.

(5) Pettersen, R. C. The Chemical Composition of Wood. *Adv. Chem. Ser.* **1984**, *207*, 57–126.

(6) Rowell, R. M.; Dietsberger, M. A. Thermal properties, combustion, and fire retardancy of wood. *Handbook of Wood Chemistry and Wood Composites*, 2nd, ed.; Rowell, R., Ed.; CRC Books, 2013; Vol. 6, pp 127–149.

(7) Nishiyama, Y. Structure and properties of the cellulose microfibril. *J. Wood Sci.* **2009**, *55*, 241–249.

(8) Wang, N.; Liu, Y.; Xu, C.; Liu, Y.; Wang, Q. Acid-base synergistic flame retardant wood pulp paper with high thermal stability. *Carbohydr. Polym.* **2017**, *178*, 123–130.

(9) Dong, Y.; Wang, K.; Li, J.; Zhang, S.; Shi, S. Q. Environmentally benign wood modifications: a review. *ACS Sustainable Chem. Eng.* **2020**, *8*, 3532–3540.

(10) Liu, L.; Qian, M.; Song, P. A.; Huang, G.; Yu, Y.; Fu, S. Fabrication of green lignin-based flame retardants for enhancing the thermal and fire retardancy properties of polypropylene/wood composites. *ACS Sustainable Chem. Eng.* **2016**, *4*, 2422–2431.

(11) Guan, Y.-H.; Huang, J.-Q.; Yang, J.-C.; Shao, Z.-B.; Wang, Y.-Z. An Effective Way to Flame-retard Biocomposite with Ethanolamine Modified Ammonium Polyphosphate and Its Flame Retardant Mechanisms. *Ind. Eng. Chem. Res.* **2015**, *54*, 3524–3531.

(12) Kumar, S. P.; Takamori, S.; Araki, H.; Kuroda, S. Flame retardancy of clay-sodium silicate composite coatings on wood for construction purposes. *RSC Adv.* **2015**, *5*, 34109–34116.

(13) Lowden, L. A.; Hull, T. R. Flammability Behaviour of Wood and a Review of the Methods for Its Reduction. *Fire Sci. Rev.* **2013**, *2*, 4.

(14) Oberley, W. J. Non-resinous, uncured tire retardant and products produced therewith. U.S. Patent 4,373,010 A, February 8, 1983.

(15) Matkó, S.; Toldy, A.; Keszei, S.; Anna, P.; Bertalan, G.; Marosi, G. Flame retardancy of biodegradable polymers and biocomposites. *Polym. Degrad. Stab.* **2005**, *88*, 138–145.

(16) Grexa, O.; Horváthová, E.; Bešinová, O. g.; Lehocký, P. Flame retardant treated plywood. *Polym. Degrad. Stab.* **1999**, *64*, 529–533.

(17) Shaw, S. D.; Blum, A.; Weber, R.; Kannan, K.; Birnbaum, L. S. Halogenated flame retardants: Do the fire safety benefits justify the risks? *Rev. Environ. Health* **2010**, *25*, 261–305.

(18) Chen, M.-J.; Xu, Y.-J.; Rao, W.-H.; Huang, J.-Q.; Wang, X.-L.; Chen, L.; Wang, Y.-Z. Influence of Valence and Structure of Phosphorus-Containing Melamine Salts on the Decomposition and Fire Behaviors of Flexible Polyurethane Foams. *Ind. Eng. Chem. Res.* **2014**, *53*, 8773.

(19) Jiang, T.; Feng, X.; Wang, Q.; Xiao, Z.; Wang, F.; Xie, Y. Fire performance of oak wood modified with N-methylol resin and methylolated guanylurea phosphate/boric acid-based fire retardant. *Constr. Build. Mater.* **2014**, *72*, 1–6.

(20) Lioudakis, S.; Vorisis, D.; Agiovlaitis, I. P. Testing the retardancy effect of various inorganic chemicals on smoldering combustion of *Pinus halepensis* needles. *Thermochim. Acta* **2006**, *444*, 157–165.

(21) Lu, S.-Y.; Hamerton, I. Recent Developments in the Chemistry of Halogen-Free Flame Retardant Polymers. *Prog. Polym. Sci.* **2002**, *27*, 1661–1712.

(22) Phromsaen, A.; Chindaprasit, P.; Hiziroglu, S.; Kasemsiri, P. Thermal Degradation and Fire Retardancy of Wood Impregnated

with Nitrogen Phosphorus Flame Retardant. *Adv. Mater. Res.* **2014**, *931–932*, 152–156.

(23) Liu, Y.; Zhao, J.; Deng, C.-L.; Chen, L.; Wang, D.-Y.; Wang, Y.-Z. Flame-retardant effect of sepiolite on an intumescent flame-retardant polypropylene system. *Ind. Eng. Chem. Res.* **2011**, *50*, 2047–2054.

(24) Genovese, A.; Shanks, R. A. Structural and thermal interpretation of the synergy and interactions between the fire retardants magnesium hydroxide and zinc borate. *Polym. Degrad. Stab.* **2007**, *92*, 2–13.

(25) Ramazani, S. A. A.; Rahimi, A.; Frounchi, M.; Radman, S. Investigation of flame retardancy and physical-mechanical properties of zinc borate and aluminum hydroxide propylene composites. *Mater. Des.* **2008**, *29*, 1051–1056.

(26) Ming, G.; Ling, B.; Yang, S. S.; Min, Z. Flame retardance of wood treated with guanidine compounds characterized by thermal degradation behavior. *J. Anal. Appl. Pyrol.* **2005**, *73*, 151–156.

(27) Jin, F.; Xia, Y.; Mao, Z.; Ding, Y.; Guan, Y.; Zheng, A. Special Spherical Shell-shaped Foam deriving from Guanidine Phosphate - Pentaerythritol system and its Intumescent Fire Retardant effects on Polypropylene. *Polym. Degrad. Stab.* **2014**, *110*, 252–259.

(28) Wang, N.; Liu, Y.; Liu, Y.; Wang, Q. Properties and mechanisms of different guanidine flame retardant wood pulp paper. *J. Anal. Appl. Pyrolysis* **2017**, *128*, 224–231.

(29) Jieyu, L.; Yinghai, C.; Caiying, S. Flame retardant of guanidine condensed phosphate (GCP) for wood. *J. For. Res.* **1994**, *5*, 58–63.

(30) Vroman, I.; Lecoeur, E.; Bourbigot, S.; Delobel, R. Guanidine hydrogen phosphate-based flame-retardant formulations for cotton. *J. Ind. Textil.* **2004**, *34*, 27–38.

(31) Goldstein, I. S.; Dreher, W. A. Method of imparting flame retardance to wood. U.S. Patent 2,917,408 A, 1959.

(32) Cummins, R. W.; Fuchs, R. J.; Thomas, J. L. Preparation of guanidine phosphate for hardboard flame retardant use. U.S. Patent. 4273687, 1981.

(33) Shen, K. K. Boron-Based Flame Retardants in Non-Halogen-Based Polymers. In *Non-Halogenated Flame Retardant Handbook*; Morgan, A. B., Wilkie, C. A., Eds.; Scrivener Publishing: MA, 2014; pp 201–241. Chapter 6.

(34) Garba, B. Effect of zinc borate as flame retardant formulation on some tropical woods. *Polym. Degrad. Stab.* **1999**, *64*, 517–522.

(35) Hu, Y. C.; Wu, Z. P.; Sun, H. Z.; Zhou, Y.; Liu, Y. Synthesis of nano zinc borate fire retardant by solid state reaction. *J. Inorg. Mater.* **2006**, *21*, 32–37.

(36) Tan, Y.; Shao, Z.-B.; Chen, X.-F.; Long, J.-W.; Chen, L.; Wang, Y.-Z. Novel Multifunctional Organic-Inorganic Hybrid Curing Agent with High Flame-Retardant Efficiency for Epoxy Resin. *ACS Appl. Mater. Interfaces* **2015**, *7*, 17919–17928.

(37) Costes, L.; Laoutid, F.; Brohez, S.; Dubois, P. Bio-based flame retardants: When nature meets fire protection. *Mater. Sci. Eng. R Rep.* **2017**, *117*, 1–25.

(38) Wei, Z.; Liu, J.; Hui, P.; Liao, J.; Wang, X. Synthesis of a novel PEPA-substituted polyphosphoramidate with high char residues and its performance as an intumescent flame retardant for epoxy resins. *Polym. Degrad. Stab.* **2015**, *118*, 120–129.

(39) Zhang, L.; Xu, J.; Shen, H.; Xu, J.; Cao, J. Montmorillonite-catalyzed furfurylated wood for flame retardancy. *Fire Saf. J.* **2021**, *121*, 103297.

(40) Li, P.; Zhang, Y.; Zuo, Y.; Lu, J.; Yuan, G.; Wu, Y. Preparation and Characterization of Sodium Silicate Impregnated Chinese Fir Wood with High Strength, Water Resistance, Flame Retardant and Smoke Suppression. *J. Mater. Res. Technol.* **2020**, *9*, 1043–1053.

(41) Hirata, T.; Kawamoto, S.; Nishimoto, T. Thermogravimetry of wood treated with water-insoluble retardants and a proposal for development of fire-retardant wood materials. *Fire Mater.* **1991**, *15*, 27–36.

(42) Wu, Z.; Shu, W.; Hu, Y. Synergist Flame Retarding Effect of Ultrafine Zinc Borate on LDPE/IFR System. *Appl. Polym. Sci.* **2000**, *103*, 3667–3674.

(43) Xu, Q.; Chen, L.; Harries, K. A.; Zhang, F.; Liu, Q.; Feng, J. Combustion and charring properties of five common constructional wood species from cone calorimeter tests. *Constr. Build. Mater.* **2015**, *96*, 416–427.

(44) Grexa, O.; Lübke, H. Flammability parameters of wood tested on a cone calorimeter. *Polym. Degrad. Stabil.* **2001**, *74*, 427–432.

(45) Byrne, C. E.; Nagle, D. C. Carbonization of wood for advanced materials applications. *Carbon* **1997**, *35*, 259–266.